J. Phys. B: At. Mol. Opt. Phys. **22** (1989) 3055-3077. Printed in the UK

Electron scattering by atomic hydrogen at intermediate energies: I. Integrated elastic, 1s–2s and 1s–2p cross sections

M P Scott, T T Scholz, H R J Walters and P G Burke

Department of Applied Mathematics and Theoretical Physics, Queen's University of Belfast, Belfast BT7 1NN, UK

Received 1 June 1989

Abstract. Integrated cross sections for 1s-1s, 1s-2s and 1s-2p electron-hydrogen-atom scattering processes are reported for scattering energies ranging from the ionisation threshold to 4 Ryd. For the total angular momentum L in the range $0 \leqslant L \leqslant 4$ the intermediate energy R-matrix theory of Burke *et al* has been used. From $L = 5$ to $L = L\max$, where $L\max$ varies between 10 and 16, calculations have been performed using the standard R-matrix close-coupling method and employing the nine-state basis (three eigenstates plus six pseudostates) of Fon *et al*. To compensate for incompleteness in the R-matrix bases, corrections have been applied to all partial waves $0 \leqslant L \leqslant L\max$ using the plane-wave second Born approximation. In addition, the second Born approximation has also been used to extrapolate the partial-wave series from $L = L\max + 1$ to infinity. The agreement with theoretical work of Callaway *et al* is good for both elastic and inelastic processes. The calculated 1s-2s and 1s-2p cross sections are in reasonable accord with experimental results originating from the 1s-2p relative data of Long *et al* independently normalised to theory at high energy and with the 2s/2p ratio measurements of Kauppila *et al*. However at 4 Ryd the 1s-2p result lies below an absolute measurement of Williams and confirms an earlier theoretical result of van Wyngaarden and Walters. Finally the total inelastic cross section is reported.

1. Introduction

The scattering of electrons by hydrogen atoms is one of the simplest processes in atomic physics. Even with the long history of studies devoted to this process there still remains uncertainty in the correct values of scattering observables including integrated cross sections (see, for example, van Wyngaarden and Walters 1986a, b). While theoreticians and experimentalists devote a good deal of effort towards determining more fundamental observables such as differential cross sections and electron-photon correlation parameters the fact remains that accurate integrated cross sections are urgently required by both the astrophysics and the plasma physics communities. It is the objective of this paper to provide these integrated cross sections. A future paper will present angular distributions and correlation parameters.

Discrepancies between various theories are particularly noticeable at intermediate scattering energies which are defined to range from the ionisation threshold to energies at which approximations based upon the Born series are applicable. In practice this upper limit is several times the ionisation threshold energy. In this energy region theoretical difficulties are not limited to electron scattering by atomic hydrogen but rather plague scattering by atoms and molecules in general. The problem at intermediate energies is that an infinite number of channels are open but they couple too strongly

0953-4075/89/193055+23$02.50

for the perturbative theories, such as those based on the Born series, to apply. Standard close-coupling methods also fail because they include only a finite number of channels in the expansion of the scattering wavefunction. This approach is unreliable when an infinite number of channels is open.

Several approaches to this problem have been developed over the last 20 years. Schlessinger and Schwartz (1966) introduced an approach based on the extrapolation of the T matrix from complex energies but they only attempted to extrapolate from real energies below the $n = 1$ threshold which was too far from the intermediate energy region to give accurate results there. Reinhardt (1979) used a basis of L^2 functions which had the advantage of avoiding specification of channels and asymptotic forms of wavefunctions. Diagonalisation of the Hamiltonian within this basis discretised the continuum spectrum from which scattering information could be obtained by extrapolation of the T matrix from complex energies onto the real energy axis (McDonald and Nuttall 1969). In practice such methods have been limited to elastic scattering. In another approach based upon low-energy close-coupling theory, the infinity of open channels omitted from the expansion of the scattering wavefunction is represented by a few well chosen pseudostates. Burke and Mitchell (1973) showed that for electron-hydrogen-atom scattering this method converged rapidly except in the neighbourhood of pseudoresonances and pseudothresholds.

The forerunner of the theory on which the present paper is based is the work of Burke *et al* (1981). They introduced a method founded upon the low-energy close-coupling expansion methods but with features of the L^2 method of Reinhardt. The scattering wavefunction is expanded in terms of the channels of interest together with a set of L^2 functions. These functions are shown to give rise to pseudoresonances at intermediate energies. They proposed that the exact T-matrix element between any states retained in the close-coupling expansion be defined by

$$T(E) = \lim_{m\to\infty} \langle T^m_{\text{approx}} \rangle_{\text{Av}} \tag{1}$$

where $\langle T^m_{\text{approx}} \rangle_{\text{Av}}$ is the energy average over pseudoresonances of an approximate T matrix evaluated in a calculation retaining m L^2 integrable functions in the expansion of the scattering wavefunction.

Burke *et al* (1981) were able to show by means of a numerical example that their procedure produced accurate results. In a similar way Slim and Stelbovics (1987) used model potentials to prove that this method does in fact converge to the correct value of the T matrix and that the order of the error of such a method applied within an R-matrix framework is a^{-1} where a is the radius of the internal R-matrix region.

The central theme of the present work is the presentation of calculations of elastic, 1s-2s and 1s-2p electron-hydrogen-atom cross sections, based upon the intermediate-energy R-matrix (IERM) theory of Burke *et al* (1987). The first stage is an extension of the IERM calculations of Scholz *et al* (1988) to include all partial waves in the range $0 \leq L \leq 4$ where L is the total orbital angular momentum. The IERM theory is an example of the type of theory introduced by Burke *et al* (1981). Its characteristic feature is the way in which the L^2 basis is defined. For scattering from a one-electron target, the expansion of the internal region wavefunction consists of the usual R-matrix bound-bound and bound-continuum terms but in addition a large set of *continuum-continuum* terms is included. The nature of the internal R-matrix region ensures that such terms are, by definition, L^2 functions. This provides a well defined and effective procedure for generating an L^2 basis which adequately spans the space of the infinity

of open channels not explicitly included in the bound-bound and bound-continuum expansion.

To compare theory with experiment it is necessary to also take account of partial waves beyond $L=4$. At higher values of L interactions are generally weaker so that methods less sophisticated than the IERM procedure, and hence computationally less expensive, should be satisfactory. We have therefore adopted the following strategy. From $L=5$ to $L=L\text{max}$, where $L\text{max}$ varies between 10 and 16 depending upon the transition and impact energy, we have made pseudostate close-coupling calculations employing a nine-state basis of three eigenstates (1s, 2s, 2p) and six pseudostates ($\overline{3}$s, $\overline{3}$p, $\overline{3}$d, $\overline{4}$s, $\overline{4}$p, $\overline{4}$d). To avoid pseudostate threshold problems two such bases were considered, the first being that of Fon *et al* (1981), the second a basis with different thresholds which we have constructed. Above $L=L\text{max}$ the second Born approximation (Kingston and Walters 1980, van Wyngaarden and Walters 1986c) has been used. The combination of IERM, pseudostate close-coupling and second Born approximation covers all partial waves from zero to infinity. The partial-wave amplitudes from the three methods join smoothly onto one another.

In the IERM and pseudostate close-coupling approximations only target states with certain angular momenta are included. For example, in the close-coupling calculations only s, p and d type pseudostates are used. Following van Wyngaarden and Walters (1986b) we have made a further refinement to our calculations by applying a correction to allow for the contribution of target states not included in the IERM and pseudostate sets. This correction term is calculated in the second Born approximation. We present numbers with and without corrections.

The plan of the paper is as follows. Section 2 describes the details of the three theoretical methods which have been employed in this work, namely IERM, pseudostate close-coupling and second Born approximation. The results of the our calculations are presented in § 3. Here comparison is made with the basic three-state 1s-2s-2p close-coupling approximation and with the more sophisticated calculations of Callaway *et al* (1987). In the latter a pseudostate wavefunction expansion has been used within a variational scheme to calculate partial-wave amplitudes for $0 \leqslant L \leqslant 3$, while for higher L a second-order optical potential method has been adopted. In § 3 we also compare our results with available experimental data. This is not straightforward because most of the experimental work needs to be corrected for cascade and polarisation effects; a careful discussion of these points is presented. Using the optical theorem we also show that our calculations allow for a substantial loss of flux into channels other than the 1s, 2s and 2p. Our conclusions are presented in § 4.

Throughout this paper atomic units (au), in which $\hbar = m_e = e = 1$, are used. The symbol a_0 denotes the Bohr radius.

2. Theory

2.1. Intermediate-energy R-matrix theory

The general electron-atom IERM scattering theory was first introduced by Burke *et al* (1987) and applied to electron-hydrogen-atom scattering in the elastic channel. It has since been applied (Scholz *et al* 1988) to elastic, 1s-2s and 1s-2p electron-hydrogen scattering processes in the $^1S^e$, $^3S^e$, $^1P^o$, $^3P^o$, $^1D^e$ and $^3D^e$ partial-wave symmetries. This work extends these calculations to include the $^1F^o$, $^3F^o$, $^1G^e$ and $^3G^e$ partial waves and

so completes the set of all waves in the range $0 \leq L \leq 4$ relevant to scattering from the ground state of the hydrogen atom. Before we discuss the details of the present application of the intermediate-energy theory it is useful to compare it with the standard R-matrix approach.

The standard R-matrix theory is an example of a close-coupling method. Details of the theory will not be given here as they may be found in a review article by Burke and Robb (1975). Basically space is divided into two regions; internal and external. The internal region is a sphere centred on the atomic nucleus just large enough to contain the initial and final target states of interest. These states are included in a close-coupling expansion. The external region is all space outside this internal region. Here the target and scattered electrons do not overlap and so to a very good approximation electron exchange and correlation may be ignored. This reduces the Schrödinger equation to a set of relatively simple single-particle coupled equations for the scattered electron. The complicated exchange and correlation effects are confined to the internal region where the scattering wavefunction is expanded in a manner which ensures that these effects are correctly accounted for.

In the case of electron scattering by atomic hydrogen the standard method expands the internal region wavefunction in terms of orbital products. These products are of two types; bound-orbital with bound-orbital products and bound-orbital with continuum-orbital products. The bound orbitals are simply the hydrogen atomic orbitals and the radial part of the continuum orbitals are numerical solutions to a simple model potential one-dimensional Schrödinger equation with logarithmic boundary conditions†. The bound-bound products are important electron correlation terms and are an essential component in the modelling of Feshbach resonances whereas the bound-continuum terms are important to both resonant and non-resonant processes because they describe the continuum electron moving in the field of the bound atom. In common with other close-coupling methods, it is well known that this standard R-matrix approach is unreliable at scattering energies above the threshold of the lowest hydrogenic target state omitted from the expansion of the wavefunction.

We may now compare this standard approach with IERM theory. The distinctive feature of the intermediate-energy theory is that it expands the internal region wavefunction not only in terms of bound-bound and bound-continuum products but also in terms of *continuum-continuum* products. The continuum-continuum terms enable the basis states of the internal region to span the *intermediate*-energy scattering wavefunction. This wavefunction, which we denote by Ψ_E, is defined by

$$(H - E)\Psi_E(\boldsymbol{r}_1, \boldsymbol{r}_2) = 0 \tag{2}$$

where H is the scattering Hamiltonian. Naturally $\Psi_E(\boldsymbol{r}_1, \boldsymbol{r}_2)$ extends over all space. If however we denote the part of Ψ_E for which both electronic coordinates lie within the internal R-matrix region by Ψ_E^{int} then unless the expansion of the R-matrix basis states includes continuum-continuum terms they cannot accurately represent Ψ_E^{int}. To illustrate the details of the intermediate-energy method we now present the calculational procedure for all partial waves in the range $0 \leq L \leq 4$.

The elastic, 1s-2s and 1s-2p electron-hydrogen-atom scattering processes are of current interest. Therefore the internal R-matrix basis states were constructed from

† See equations (3) and (4).

the bound 1s, 2s and 2p hydrogen atom orbitals along with members of a complete set of continuum orbitals. Allowance was made for the truncation of the complete set through the inclusion of a Buttle correction (Buttle 1967). Denoting the radial part of both the bound hydrogenic orbitals and the continuum orbitals by $u_{nl}(r)$ where n and l are the principal and angular momentum quantum numbers respectively, the continuum orbitals $u_{nl}(r)$ are numerically generated for each l by solving the following standard R-matrix radial equation:

$$\left(\frac{d^2}{dr^2}-\frac{l(l+1)}{r^2}+V(r)+k_{nl}^2\right)u_{nl}(r)=\sum_{n'=l+1}^{2}\lambda_{nln'l}u_{n'l}(r) \tag{3}$$

with boundary conditions

$$u_{nl}(0)=0 \qquad du_{nl}(r)/dr|_{r=a}=0 \tag{4}$$

where a is the radius of the internal R-matrix region and $\lambda_{nln'l}$ are Lagrange multipliers which ensure that the $u_{nl}(r)$ functions are orthogonal to the bound orbitals of the same symmetry. The $V(r)$ term should model as closely as possible the potential experienced by the scattering electron to ensure rapid convergence of the numerical orbital set. With this in mind it was chosen as the static hydrogen atom potential. Equations (3) and (4) are identical to those of the standard R-matrix theory.

The R-matrix basis states for each partial-wave symmetry defined by total angular momentum L, total spin angular momentum S and parity π quantum numbers are given by

$$\Theta_k^{LS\pi}(\boldsymbol{r}_1,\boldsymbol{r}_2)=\sum_{n_1n_2}^{n\max}\sum_{l_1}^{l1\max}\sum_{l_2}^{l2\max}\Phi_{n_1l_1n_2l_2}^{LM_L}(\boldsymbol{r}_1,\boldsymbol{r}_2)\alpha_{n_1n_2l_1l_2k}^{LS\pi}. \tag{5}$$

The $\Phi_{n_1l_1n_2l_2}^{LM_L}$ basis states are defined by

$$\Phi_{n_1l_1n_2l_2}^{LM_L}(\boldsymbol{r}_1,\boldsymbol{r}_2)=(1+(-1)^S P_{12})r_1^{-1}u_{n_1l_1}(r_1)r_2^{-1}u_{n_2l_2}(r_2)\mathcal{Y}_{l_1l_2LM_L}(\hat{\boldsymbol{r}}_1,\hat{\boldsymbol{r}}_2) \tag{6}$$

where P_{12} is the antisymmetry space exchange operator. The angular functions $\mathcal{Y}_{l_1l_2LM_L}(\hat{\boldsymbol{r}}_1,\hat{\boldsymbol{r}}_2)$ which are eigenfunctions of L^2, L_z, l_1^2 and l_2^2 are generated in the usual way, taking expansions of products of spherical harmonics weighted with Clebsch-Gordan coefficients. The α coefficients are determined by diagonalisation of the two-electron Hamiltonian in the internal region. Naturally this expansion must be terminated with finite values of $n$max, $l1$max and $l2$max. Comparison of the R-matrix eigenvalues with the range of scattering energies under consideration made it clear that a value of $n$max equal to 30 was sufficient for each partial wave. Small errors resulting from the truncation of the n_1 and n_2 to 30 are taken into account through the Buttle correction to the diagonal elements of the R-matrix. The same cannot be said for the truncation of the angular momentum quantum numbers l_1 and l_2. A constraint on the (l_1, l_2) combinations included in the $\Theta_k^{LS\pi}$ expansion was the computing facilities which limited the dimension of the Hamiltonian and hence number of $\Phi_{n_1l_1n_2l_2}^{LM_L}$ basis states to 3500. From table 1 which lists the resulting number of basis states for each partial wave it is clear that both F and G waves have almost reached

Table 1. Total number of $\Phi_{n_1l_1n_2l_2}^{LM_L}$ basis states for each symmetry.

Symmetry	$^1S^e$	$^3S^e$	$^1P^o$	$^3P^o$	$^1D^e$	$^3D^e$	$^1F^o$	$^3F^o$	$^1G^e$	$^3G^e$
No of states	1306	1219	2438	2438	2842	2758	3132	3132	3422	3394

this limit and so additional (l_1, l_2) combinations cannot be included. Another influence on the number of (l_1, l_2) combinations which may be included is the symmetry relations existing for $l_1 = l_2$ combinations which have the effect of reducing the number of $\Phi^{LM_L}_{n_1 l_1 n_2 l_2}$ basis states. For example, from table 2 which lists all (l_1, l_2) contributions which we included in the expansion of $\Theta_k^{LS\pi}$ it is clear that the D waves include more combinations than the F waves. However it is evident from table 1 that the total number of basis states for the D waves is less than for the F waves. This is because symmetry relations reduce the number of $\Phi^{LM_L}_{n_1 l_1 n_2 l_2}$ D wave states originating from the $(l_1, l_2) = (1, 1)$, $(2, 2)$ and $(3, 3)$ combinations. A plane-wave second Born calculation for the contribution of the infinity of omitted (l_1, l_2) terms is presented in § 2.3.2. The results of these calculations show that the corrections for such terms are relatively small, indicating that our R-matrix basis state expansion includes the most dominant (l_1, l_2) combinations.

Table 2. Angular momentum of orbitals retained in R-matrix basis state expansion.

$^1S^e, ^3S^e$		$^1P^o, ^3P^o$		$^1D^e, ^3D^e$		$^1F^o, ^3F^o$		$^1G^e, ^3G^e$	
l_1	l_2	l_1	l_2	l_1	l_2	l_1	l_2	l_1	l_2
0	0	0	1	0	2	0	3	0	4
1	1	1	2	1	1	1	2	1	3
2	2	2	3	1	3	1	4	1	5
				2	2	2	3	2	2
				3	3			2	4

As in the standard theory the internal R-matrix region must be large enough to envelop the hydrogen target states involved in any transitions under consideration. Therefore in the present study the 1s, 2s and 2p eigenstates must be fully included. From the analytic expressions for the radial parts of these states a boundary radius of 25 a_0 was deemed sufficient. Diagonalisation of the Hamiltonian within the $\Phi^{LM_L}_{n_1 l_1 n_2 l_2}$ basis yielded an energy-dependent R matrix in the usual manner. With Buttle terms added to the diagonal elements, these R matrices were used to obtain the K matrices (from which all scattering observables may be deduced) by matching onto an asymptotic expansion at the $25a_0$ boundary with the aid of an asymptotic package (Noble and Nesbet 1984) allowing only for 1s, 2s and 2p channels. The K matrices were obtained at 0.002 Ryd increments for scattering energies ranging from threshold to 6 Ryd. The R matrices are used in the matching process because they represent the ratio of that part of the wavefunction which describes the scattered electron to its derivative, both evaluated at the R-matrix boundary. Although the full polarisability was represented in the internal region, the asymptotic form of the wavefunction includes just the 1s, 2s and 2p states of the hydrogen atom which only account for 66.5% of the static polarisability of the hydrogen atom in its ground state. The remaining 33.5% was therefore inserted into the 1s–1s element of the r^{-4} asymptotic coefficient matrix.

We mentioned briefly in the introduction that the inclusion of the continuum–continuum terms in the expansion of the wavefunction gives rise to pseudoresonances at intermediate energies and that the physical T-matrix element may be obtained by energy averaging the approximate T matrix over these resonances. The energy interval I over which the averaging is taken must be large compared with the pseudoresonance width but small on the scale of significant variations in the gradient of the background

T matrix. Burke *et al* (1981) took the averaging function to be the Lorentizian function

$$\rho(E-E')=\frac{I}{\pi}\frac{1}{(E-E')^2+I^2}. \tag{7}$$

It is well known that T matrices do not have poles on the physical sheet in the upper half complex energy plane. It is therefore trivial to show that for the average of a T-matrix element

$$\langle T(E)\rangle_{\mathrm{Av}}=\int_{-\infty}^{\infty}\rho(E-E')T(E')\,\mathrm{d}E'=T(E+\mathrm{i}I). \tag{8}$$

In the limit $m\to\infty$ and $a\to\infty$ the width and distance between the poles tends to zero so it is possible to let $I\to 0$. From (8) it is clear that as $I\to 0$ the averaging procedure corresponds to evaluating the T matrix just above the branch cut on the real energy axis. We found that the averaged T-matrix elements were insensitive to the width I of the averaging function. So in this work it was not necessary to take the limit $I\to 0$ to obtain the physical T-matrix element.

In practice the width and separation of the pseudoresonances arising in our calculations were hundredths of a Ryd for all channels. So the width I of the averaging function $\rho(E-E')$ ranged from 0.35 to 0.5 Ryd depending on the channel considered. The convolution described in (8) was implemented above the ionisation threshold but not below because it was found that the gradient of the background T matrix generally varied quite rapidly up to the ionisation threshold. In this situation convolution would produce inaccurate results. The complete averaging procedure for each of the real and imaginary T-matrix elements of channels relevant to partial waves in the range $0\leqslant L\leqslant 4$ is described in the following steps.

(1) The T-matrix element was convolved with the Lorentizian function $\rho(E-E')$ for energies ranging from the ionisation threshold to about 5.5 Ryd. In practice the tails of ρ had to be truncated. The resultant averaged T matrix characteristically contained oscillations of very small amplitude imposed upon a smooth background.

(2) A least-squares cubic spline fit was then made to the entire T-matrix element consisting of the unaveraged function from the channel threshold to the ionisation threshold, the convolved function obtained in step (1) from the ionisation threshold to about 5.5 Ryd and finally the unaveraged T matrix from 5.5 to 6 Ryd. The cubic spline fit was forced to match smoothly onto the T-matrix element in the 0.75–0.85 Ryd low-energy region. This region is free of pseudoresonances and so we expect the T matrix to be physically accurate. At the 6 Ryd high-energy limit the T matrix is dominated by pseudoresonances so the spline cannot match in a similar way. Instead it is forced to terminate as a quadratic which ensures that the fitted curve is well behaved in the high-energy limit. About four cubic spline knots are required over the entire energy range.

The overall effect of the cubic spline least-squares fitting procedure of step (2) was to smooth the unconvoluted pseudoresonances existing below the ionisation threshold and above 5.5 Ryd and to remove the small oscillations in the convolved region. An example of the results of this averaging procedure is given in figure 1 which plots the imaginary part of the elastic $^1\mathrm{D}^e$ partial-wave T-matrix element. It is clear from the figure that the fitting procedure commences at an energy above the physical $(2\mathrm{p})^2$ resonance leaving it completely undisturbed. Another example can be found in the work of Scholz *et al* (1988).

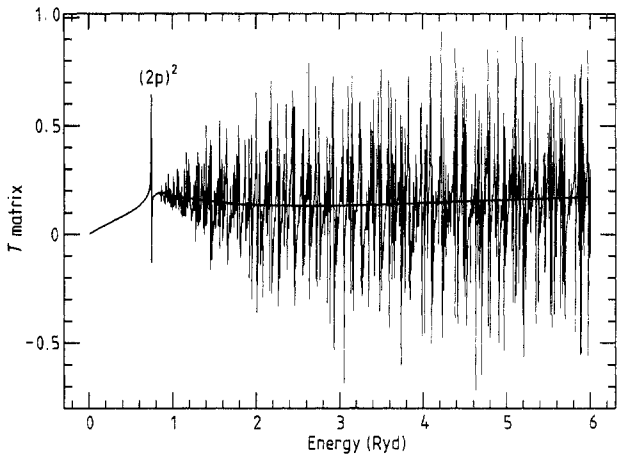

Figure 1. Results of the averaging procedure applied to the imaginary part of the elastic $^1D^e$ partial-wave T-matrix element.

To conclude this section we emphasise that this averaging procedure represents the loss of flux into all the highly excited and continuum states not explicitly included in the external region. The resultant averaged S matrix $\langle S(E)\rangle_{Av} = \langle T(E)\rangle_{Av} + 1$, unlike the S matrix $S(E)$ before averaging, is not unitary and can be used to obtain an accurate estimation of the total cross section including the ionisation cross section. This estimate is presented in § 4.

2.2. Nine-state close coupling

Partial-wave amplitudes in the range $5 \leq L \leq L\text{max}$ were evaluated within the framework of the standard R-matrix theory. To account for the effect of the infinite number of channels open at intermediate energies the set of target states upon which the close-coupling expansion of the internal R-matrix region was based included not only the 1s, 2s and 2p eigenstates but also a set of pseudostates. As far as the calculational procedure was concerned these pseudostates take on a role equivalent to the eigenstates. That is to say they were included as target states in the internal-region close-coupling expansion and also formed channels in the expansion of the external region wavefunction. The pseudostates are important to intermediate energy scattering for the following reasons. Firstly their inclusion assists the close-coupling expansion of the internal region to span the space of the scattering wavefunction. Secondly the couplings between eigenstate and pseudostate channels in the external region model in some average way the couplings of the 1s, 2s and 2p eigenstates to the infinity of omitted channels.

As mentioned in the introduction we performed two groups of calculations each utilising a different set of pseudostates. The goal was to ensure that the final integrated cross sections were insensitive to pseudothreshold effects. One basis set was identical to that used by Fon *et al* (1981) which included the 1s, 2s and 2p eigenstates along with pseudostates labelled $\overline{3s}$, $\overline{3p}$, $\overline{3d}$, $\overline{4s}$, $\overline{4p}$ and $\overline{4d}$ where the number refers to the principal quantum number and s, p and d to the angular momentum symmetry. Fon and co-workers generated their pseudostates using the following criteria.

(1) The atomic 1s, 2s and 2p eigenstates and pseudostates form an orthonormal set.

(2) The coupling between the 1s and p states gives the full polarisability of the ground state.

(3) All pseudostates have a similar range to the $n = 2$ eigenstates.

(4) The $n = 3$ pseudostates are degenerate, to ease computational difficulties in the external region.

To test for the effect of pseudothresholds on integrated cross sections we generated a pseudostate basis similar to that of Fon *et al* but with different pseudothresholds. The criteria for the generation of our set were identical to the above list except that the effect of moving pseudothresholds was to force the relaxation of criterion number 2. However this criterion is not important for intermediate-energy scattering. Table 3 lists the thresholds for both basis sets.

Table 3. The thresholds in Ryd for the two pseudostate bases used in the calculation of partial waves satisfying $5 \leqslant L \leqslant L\text{max}$.

s states			p states			d states		
	Energy (Ryd)			Energy (Ryd)			Energy (Ryd)	
State	Fon	This work	State	Fon	This work	State	Fon	This work
1s	−1.0	−1.0	—	—	—	—	—	—
2s	−0.25	−0.25	2p	−0.25	−0.25	—	—	—
$\overline{3}$s	0.0	0.05	$\overline{3}$p	0.0	0.05	3d	0.0	0.05
$\overline{4}$s	1.5118	1.9613	$\overline{4}$p	1.0509	1.3655	$\overline{4}$d	0.9454	1.2615

We have calculated our integrated cross sections using both the Fon nine-state basis and our own nine-state basis in the range $5 \leqslant L \leqslant L\text{max}$. Very good agreement was found between the two sets of numbers. In fact over the entire energy region from the ionisation threshold to 4 Ryd the elastic cross section differed at most by only 0.2%, the 1s-2s one by 1.5% and the 1s-2p one by 1.0%. However agreement was a good deal better than this at most energies. We conclude that the final cross sections reported in § 3, which have been calculated with the Fon nine-state basis for $5 \leqslant L \leqslant L\text{max}$, should have no substantial errors arising from pseudothreshold effects.

It is of interest to compare the pseudostate results for the scattering amplitude with the corresponding IERM values at the changeover point $L = 4$ between the two methods. Figure 2 plots a typical example, in this case the imaginary part of the T-matrix element for the 1s-2p ($l = L - 1$ for the scattered electron) channel of the $^1G^e$ partial wave. It is seen that the Fon nine-state calculation produces an amplitude containing several pseudoresonances (i.e. unphysical resonances). If, following Burke *et al* (1981), we imagine a smooth fit through the pseudoresonances of the nine-state calculation we see that good agreement would be obtained with the IERM theory. Above $L = 4$ where we actually use the nine-state approximation there are no pseudoresonances arising from the pseudostates†. This along with the average agreement with the IERM approximation illustrated in figure 2 lends weight to the supposition that for $L > 4$ the nine-state calculations are sufficiently accurate.

Continuity between the T-matrix elements as L increases is another important criterion which any hybrid of approximations, as here, should satisfy. A typical example

† The pseudostate basis contains states of s, p and d symmetry only. No two of these can be combined to produce an L^2 function with an overall symmetry of $L \geqslant 5$.

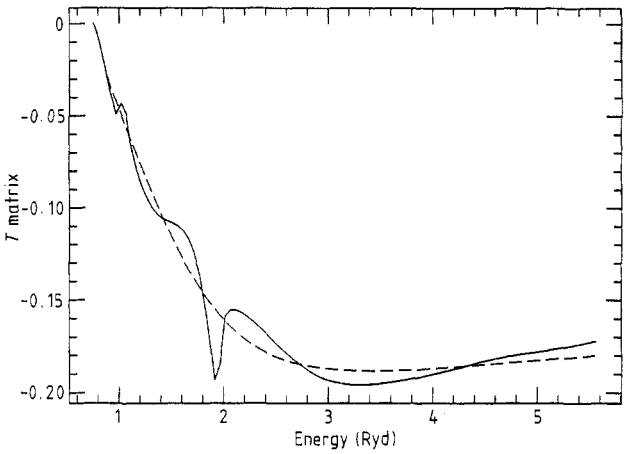

Figure 2. Imaginary part of the T matrix for the 1s-2p ($l = L-1$ for scattered electron) channel of the $^1G^e$ partial wave. Full curve, Fon nine-state calculation; broken curve, intermediate-energy R-matrix theory.

is shown in figure 3. Here we plot the real part of the 1s-2p ($l = L-1$ for scattered electron) T-matrix elements for triplet scattering at 4.0 Ryd. The smooth behaviour in the elements across the value $L = 4$, where we change over from the IERM theory to the Fon nine-state approximation, should be noted. This lends further confidence to our use of the nine-state approximation above $L = 4$.

2.3. Second Born approximation

In this work the plane-wave second Born approximation is used in two ways: firstly, as a means of extrapolating the partial-wave series for the amplitudes from $L = L\max + 1$

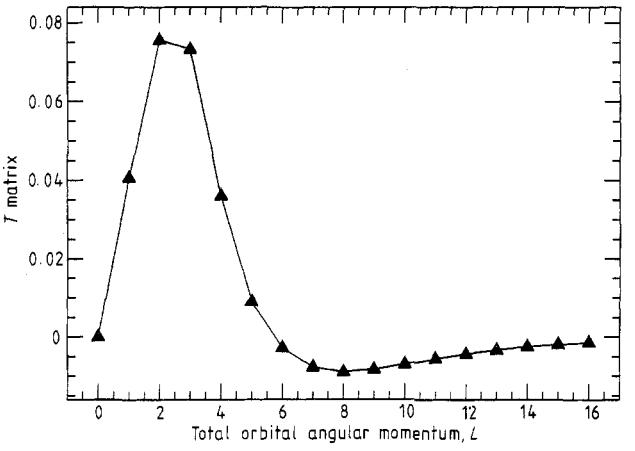

Figure 3. Real part of the 1s-2p ($l = L-1$ for scattered electron) T-matrix elements for triplet partial waves calculated as a function of total orbital angular momentum at a scattering energy of 4.0 Ryd. Results for $0 \leqslant L \leqslant 4$ obtained using the IERM method; results for $5 \leqslant L \leqslant 16$ obtained using the pseudostate method.

to infinity; secondly, as a method of applying a correction to the IERM and Fon nine-state approximations to make allowance for (l_1, l_2) combinations and target states omitted from the expansion of the wavefunction. The plane-wave second Born amplitudes we employ have all been calculated in the closure approximation in the manner described by Kingston and Walters (1980).

2.3.1. Extrapolation of the partial-wave series beyond $L = Lmax$. The method we use is that given by van Wyngaarden and Walters (1986c). For simplicity the procedure is described only for an s-s transition, the generalisation to s-p transitions is obvious.

Following the notation of Walters (1984), let f^{Born2} be the full plane-wave second Born amplitude, i.e. the sum of the first Born term f^{B1} and the second Born term f^{B2}. This amplitude may be expanded in partial waves according to

$$f^{\text{Born2}} = \frac{-\text{i}}{2\sqrt{k_0 k_f}} \sum_{L=0}^{\infty} (2L+1) T_L^{\text{Born2}} P_L(\cos\theta) \tag{9}$$

where θ is the scattering angle, T_L^{Born2} is the second Born partial-wave T-matrix element, k_0 and k_f are the momenta of the incident and scattered electrons and P_L is a Legendre polynomial. Let T_L^S ($S = 0$ for singlet, $S = 1$ for triplet) be the corresponding partial-wave amplitudes calculated in the IERM approximation for $0 \leqslant L \leqslant 4$ and in the nine-state pseudostate close-coupling approximation for $5 \leqslant L \leqslant Lmax$. The value of $Lmax$ is always such that exchange is negligible there, i.e. $T_{Lmax}^0 \simeq T_{Lmax}^1$.

Let f^S be the full amplitude for the transitions considered. We take

$$f^S = \frac{-\text{i}}{2\sqrt{k_0 k_f}} \sum_{L=0}^{Lmax} (2L+1) T_L^S P_L(\cos\theta) + \frac{-\text{i}}{2\sqrt{k_0 k_f}} \sum_{L=Lmax+1}^{\infty} (2L+1)[\alpha^S \,\text{Re}(T_L^{\text{Born2}}) + \text{i}\beta^S \,\text{Im}(T_L^{\text{Born2}})] P_L(\cos\theta) \tag{10}$$

where

$$\alpha^S \equiv \text{Re}(T_{Lmax}^S)/\text{Re}(T_{Lmax}^{\text{Born2}}) \qquad \beta^S \equiv \text{Im}(T_{Lmax}^S)/\text{Im}(T_{Lmax}^{\text{Born2}}). \tag{11}$$

The prescription (10) amounts to scaling (usually slight) of the second Born approximation so as to match the nine-state calculations at $L = Lmax$. Using (9), (10) can be expressed in terms of f^{Born2} and a finite partial-wave sum from zero to $Lmax$ (see van Wyngaarden and Walters 1986c).

2.3.2. Correction for omissions in the IERM and pseudostate calculations. The IERM calculations are restricted to a finite number of (l_1, l_2) combinations while the nine-state pseudostate close-coupling approximation only employs target states of s, p and d types. Following van Wyngaarden and Walters (1986b) we have used the plane-wave† second Born approximation to represent the omitted target states. (i.e. f, g, h etc) for $5 \leqslant L \leqslant Lmax$ and the omitted (l_1, l_2) combinations for $0 \leqslant L \leqslant 4$.

The second Born term has the form (see Walters 1984 for notation)

$$f^{\text{B2}} = -\frac{1}{8\pi^4} \sum_n \int \text{d}\boldsymbol{k} \frac{\langle \boldsymbol{k}_f \psi_f | V | \boldsymbol{k} \psi_n \rangle \langle \boldsymbol{k} \psi_n | V | \boldsymbol{k}_0 \psi_0 \rangle}{k_n^2 - k^2 + \text{i}\eta} \tag{12}$$

† Note that van Wyngaarden and Walters actually used the distorted-wave second Born approximation in their work; here we have only used the plane-wave approximation.

where the limit $\eta \to 0+$ is to be understood. In (12) the ψ_n are the hydrogen eigenstates, ψ_0 and ψ_f being the initial and final states. In the present work (12) is calculated in the closure approximation (Kingston and Walters 1980). Each term in the formula (12) may be interpreted as involving a virtual transition of the atom from the state ψ_0 to intermediate state ψ_n and back again to ψ_f. At the same time the incident electron is scattered from $\boldsymbol{k}_0$ into the virtual intermediate plane-wave state $\boldsymbol{k}$ and back again to $\boldsymbol{k}_f$.

For notational simplicity let us again assume that ψ_0 and ψ_f are both s states. Then f^{B2} may be expanded in partial waves according to

$$f^{\mathrm{B2}} = \frac{-\mathrm{i}}{2\sqrt{k_0 k_f}} \sum_{L=0}^{\infty} (2L+1) T_L^{\mathrm{B2}} P_L(\cos\theta). \tag{13}$$

Each element T_L^{B2} may be further decomposed into

$$T_L^{\mathrm{B2}} = \sum_{l_T=0}^{\infty} \sum_{\substack{l_1=|L-l_T| \\ (\text{in steps of } 2)}}^{L+l_T} T_L^{\mathrm{B2}}(l_T, l_1) \tag{14}$$

where $T_L^{\mathrm{B2}}(l_T, l_1)$ represents the contribution to T_L^{B2} from all intermediate target states ψ_n with angular momentum l_T and where the incident electron in the intermediate plane wave state $\boldsymbol{k}$ has angular momentum l_1†. For example, if ψ_n is a d state ($l_T = 2$) then l_1 is $L-2$, L or $L+2$.

To correct the IERM amplitudes T_L^S ($0 \leqslant L \leqslant 4$) for the omitted (l_1, l_2) contributions we write

$$T_L^S(\text{corrected}) = T_L^S + T_L^{\mathrm{B2}} - \sum_{\substack{l_T, l_1 \\ \text{IERM combinations } (l_1, l_2)}} T_L^{\mathrm{B2}}(l_T, l_1). \tag{15}$$

In the sum the pair (l_T, l_1) must range over all distinct combinations of (l_1, l_2) *and*‡ (l_2, l_1) which have been used for the IERM calculation of T_L^S. For example, for the F waves of table 2 (l_T, l_1) in the sum (15) takes on the values (0, 3), (1, 2), (1, 4), (2, 1), (2, 3), (3, 0), (3, 2) and (4, 1).

In the range of the nine-state calculations, $5 \leqslant L \leqslant L_{\max}$, the corrected amplitude is

$$T_L^S(\text{corrected}) = T_L^S + T_L^{\mathrm{B2}} - \sum_{l_T=0}^{2} \sum_{\substack{l_1=|L-l_T| \\ (\text{in steps of } 2)}}^{L+l_T} T_L^{\mathrm{B2}}(l_T, l_1). \tag{16}$$

The final corrected full amplitude is then

$$f^S(\text{corrected}) = \frac{-\mathrm{i}}{2\sqrt{k_0 k_f}} \sum_{L=0}^{L\max} (2L+1) T_L^S(\text{corrected}) P_L(\cos\theta) - \frac{\mathrm{i}}{2\sqrt{k_0 k_f}} \sum_{L=L\max+1}^{\infty} (2L+1)[\alpha_c^S \,\mathrm{Re}(T_L^{\mathrm{Born2}}) + \mathrm{i}\beta_c^S \mathrm{Im}(T_L^{\mathrm{Born2}})] P_L(\cos\theta) \tag{17}$$

where the second sum comes from the second Born extrapolation discussed in § 2.3.1 and where now (see (10) and (11))

$$\alpha_c^S \equiv \mathrm{Re}(T_{L\max}^S(\text{corrected}))/\mathrm{Re}(T_{L\max}^{\mathrm{Born2}}) \qquad \beta_c^S \equiv \mathrm{Im}(T_{L\max}^S(\text{corrected}))/\mathrm{Im}(T_{L\max}^{\mathrm{Born2}}). \tag{18}$$

† A detailed example of such a decomposition may be found in § 4.3 of Walters (1984) where $l \equiv l_T$ and $\lambda \equiv l_1$.
‡ Our second Born approximation takes account only of direct scattering, not of exchange scattering. In the IERM expansion direct scattering proceeds through both $l_T = l_1$, $l_1 = l_2$ and $l_T = l_2$, $l_1 = l_1$.

2.4. Calculation of cross sections

Once the full scattering amplitude has been constructed, see (10) and (16), the corresponding spin averaged differential cross section, $d\sigma/d\Omega$, is calculated from

$$d\sigma/d\Omega = (k_f/4k_0)(|f^0|^2+3|f^1|^2) \tag{19}$$

and integrated to produce the integrated cross section

$$Q(0-f) = \int \frac{d\sigma}{d\Omega} d\Omega. \tag{20}$$

We shall also be interested in seeing what fraction of $Q(0-f)$ comes from a particular angular momentum range $0 \leqslant L \leqslant L'$, say. This is most readily achieved by using the formula

$$Q'(0-f) = \frac{\pi}{4k_0^2} \sum_{L=0}^{L'} (2L+1) \sum_{l=|L-l_f|}^{L+l_f} (|T_{Ll}^0|^2+3|T_{Ll}^1|^2) \tag{21}$$

where l_f is the angular momentum of the final state ψ_f and where the index l on T_{Ll} indicates angular momentum of the scattered electron in the final state†. Note that in this paper ψ_0 is always the ground 1s state.

3. Results

3.1. Introduction

Our results span the energy range from the ionisation threshold (13.6 eV) to 4 Ryd (54.4 eV). At this upper limit the $n = 2$ cross sections are in very good agreement with the higher energy calculations of van Wyngaarden and Walters (1986b)‡. The two sets of results together span an energy range from 13.6 to 350 eV, which may be further extended to 680 eV by using the distorted-wave second Born numbers of Kingston and Walters (1980).

The 4 Ryd energy point is particularly interesting for here we find the only absolute measurement of an electron-hydrogen integrated cross section, namely the 1s-2p cross section (Williams 1981). This measurement is in agreement with the simple 1s-2s-2p three-state close-coupling approximation and was also supported by later more sophisticated pseudostate calculations of Callaway (1985) and Bransden *et al* (1985). However, contrary to this accord, van Wyngaarden and Walters (1986b) obtained a result in significant disagreement with the measurement; these authors further showed that if the earlier relative experimental data of Long *et al* (1968) were normalised to theory at 200 eV, where theory should be very accurate, then the normalised data supported their calculated cross section at 54.4 eV and therefore disagreed with William's absolute measurement. Van Wyngaarden and Walters (1986a) later went on to demonstrate that the theoretical numbers of Callaway (1985) and Bransden *et al* (1985) were too large. They identified the problem as arising from two sources: the first, and main, source was the use of insufficiently accurate approximations to evaluate the higher partial-wave amplitudes; the second concerned the importance of including a good

† Note that in formulae (9), (10) and (13) to (18) it was assumed, for simplicity of explanation, that ψ_f was an s state, then $l = L$ and we denote T_{LL}^S simply as T_L^S.

‡ For elastic scattering van Wyngaarden and Walters begin their calculations at 100 eV.

description of d-type target states in the calculations. Taking the results of Callaway (1985), van Wyngaarden and Walters (1986a) applied a correction to this work to allow for the above two effects and were then able to show that the corrected 1s-2p cross sections were in quite good agreement with the normalised relative measurements of Long *et al* (1969) over a wide energy range, 13.4 to 200 eV. Finally, the more recent work of Callaway *et al* (1987) confirms the diagnosis of the 1s-2p cross section given by van Wyngaarden and Walters (1986a).

The even more refined calculations of this paper again indicate that the absolute measurement of the 1s-2p cross section is too large. We have also performed quite meticulous comparison with the relative experimental data of Long *et al* (1968), giving very careful consideration to cascade and polarisation effects. Like van Wyngaarden and Walters (1986a, b) we found quite good agreement with these data. The absolute measurement at 54.4 eV therefore remains increasingly isolated.

3.2. Comparisons

Our cross sections $Q(0-f)$ for elastic scattering, 1s-2s and 1s-2p excitations are shown in figures 4, 5 and 6. Unless otherwise stated these have been calculated using the corrected scattering amplitude (17).

Also shown in figures 4, 5 and 6 are the same cross sections evaluated using the $0 \leqslant L \leqslant 4$ IERM partial waves only†, see (21); these cross sections we denote as $Q^4(0-f)$. Comparison of Q with Q^4 reveals what fraction of the cross section comes from the very reliable IERM approximation. Figure 4 shows that over the entire energy range the elastic cross section comes almost exclusively from the accurate IERM calculations. The same is true for $n=2$ excitation near the ionisation threshold, figures 5 and 6; however, at higher energies only 75% of the 1s-2s cross section arises from these lower partial waves and for the 1s-2p scattering the contribution falls to about 25% at the 4 Ryd high-energy limit.

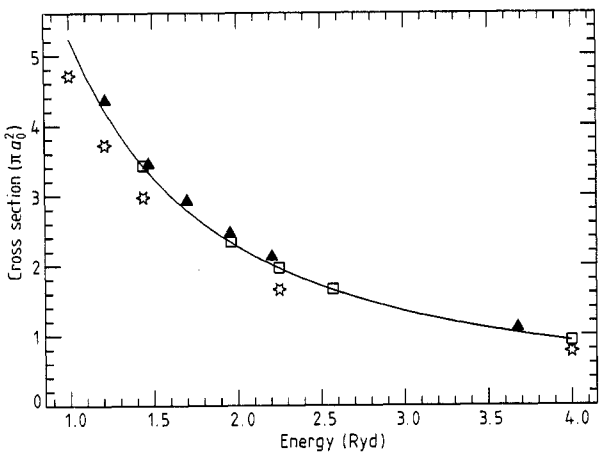

Figure 4. Theoretical elastic integrated cross sections. Full triangles, this work; full curve, sum of partial-wave cross sections $L=0$-4; stars, 1s-2s-2p close coupling; open squares, Callaway *et al* (1987).

† The second Born corrections for the omitted (l_1, l_2) combinations, § 2.3.2, have not been applied in this case.

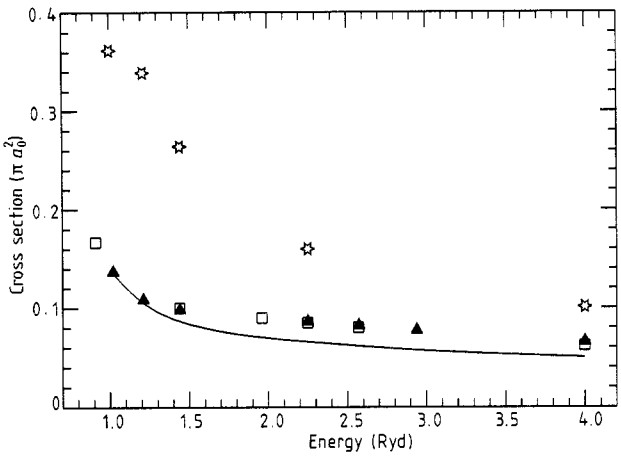

Figure 5. Theoretical 1s–2s integrated cross sections. Symbols in common with figure 4 refer to the same data.

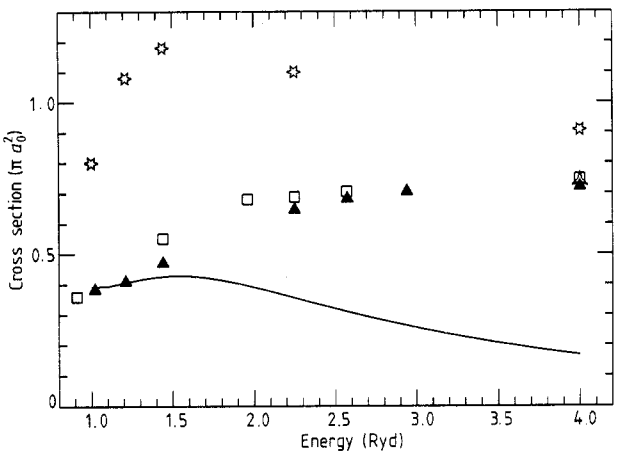

Figure 6. Theoretical 1s–2p integrated cross sections. Symbols in common with figure 4 refer to the same data. Three point star at 4 Ryd, van Wyngaarden and Walters (1986b).

In figures 4, 5 and 6 we also show results calculated in the three-state 1s–2s–2p close-coupling approximation (Burke *et al* 1963, Kingston *et al* 1976). As might be expected of a theory which ignores the effect of the infinity of channels open at intermediate energies agreement with our results is poor. This is particularly so for inelastic processes where the cross section is more than a factor of two high at some energies.

In contrast the more sophisticated calculations of Callaway *et al* (1987) are in good agreement with our work. For partial waves in the range $0 \leqslant L \leqslant 3$ Callaway *et al* used a variational close-coupling approach with a basis of 1s, 2s, 2p and 3d atomic eigenstates along with a set of seven pseudostates which included s, p and d symmetries. This approach is similar to the Fon nine-state close-coupling method. These calculations gave rise to rather broad pseudoresonances which Callaway *et al* averaged using the

T-matrix averaging procedure of Burke *et al* (1981). Our present calculations are more extensive and refined than those of Callaway *et al* in the important region $0 \leqslant L \leqslant 4$. Firstly, even without the additional second Born corrections of § 2.3.2 for omitted states, our *R*-matrix basis state expansion for $0 \leqslant L \leqslant 4$ should span intermediate-energy scattering wavefunctions more completely; inclusion of the second Born corrections further increases the accuracy of this work. Secondly, our pseudoresonances were very much narrower and denser than those of Callaway *et al*, which reduces the uncertainty due to *T*-matrix averaging. For $L \geqslant 4$ Callaway *et al* have employed a 1s-2s-2p-3s-3p-3d close-coupling approximation supplemented with a second-order perturbative non-exchange optical potential to allow for the effect of the remaining infinity of open channels. For $5 \leqslant L \leqslant L\text{max}$ ($L\text{max} = 10$–16) our treatment is non-perturbative and makes full allowance for exchange, i.e. we perform pseudostate close coupling using the Fon nine-state basis. This calculation is further refined by using the second Born approximation to account for target states of angular momenta not included in the nine-state set (§ 2.3.2). For $L > L\text{max}$ we use the straight second Born approximation. That the extra refinements of the present work lead to cross sections not greatly different from the results of Callaway *et al* (1987) encourages us to believe that we are very close to exact cross sections.

At 4 Ryd we can compare with the higher-energy calculations of van Wyngaarden and Walters (1986a). Our results are in very good agreement with their values. In particular, this confirms their 1s-2p cross section (figure 6) which was the first calculation to show disagreement with the absolute measurement of Williams (1981). For the 1s-2s transition their result is so close to our value that we have omitted it from figure 5.

There has not been a great deal of experimental investigation of integrated cross sections for electron-hydrogen-atom scattering. The data which do exist come almost exclusively from experiments performed prior to 1971. The sparse literature is largely due to the difficulty of obtaining good quality hydrogen-atom sources and the fact that in the 1970s when hydrogen atom scattering experiments became more common, attention shifted from measuring integrated cross sections to more fundamental observables such as differential cross sections and electron-photon coincidence parameters. In fact as far as we are aware only one direct experimental integrated cross section measurement (Williams 1981) has been performed at intermediate energies in the last 17 years.

Integrated 1s-2s and 1s-2p cross sections have been measured experimentally by observing Lyman-α photons emitted when the hydrogen atoms decay back into their ground states after electron impact excitation. This method is clearly not available to elastic scattering experiments and as far as we know the elastic scattering integrated cross section has never been measured directly. In the $n = 2$ excitation experiments the hydrogen atoms excited to a 2p state decay almost instantaneoulsy emitting a Lyman-α photon. The metastable 2s atoms are passed through quenching plates positioned well away from the collision region. Detection of Lyman-α photons emitted from between these plates enables the production rate of 2s atoms to be determined.

An unfortunate consequence of this experimental procedure is that at intermediate energies Lyman-α photons arise not only from direct $n = 2$ excitation but also from cascade to the $n = 2$ levels. The following illustrates just one of the many possible cascade routes to the 2p state.

$$e^- + H(1s) \rightarrow e^- + H(3s) \rightarrow e^- + H(2p) + \gamma. \tag{22}$$

The resulting 2p atom decays emitting the Lyman-α photon. Allowance for cascade

processes must be included prior to comparison between theory and experiment. As no experimental data exist for these processes theoretical results must be employed.

Another consideration is the anisotropy of the radiation emitted from the decaying hydrogen atoms. Most experiments position the photon detector at an angle of 90° to both the incident electron and hydrogen-atom beams. With this geometry the cross section inferred from photon counting data will not be correct unless the anisotropy of the Lyman-α radiation is properly accounted for. Denoting the experimental cross section obtained by assuming isotropic emission as $Q_\perp$ then the actual Lyman-α cross section (which includes cascade) is given by

$$Q = (1 - \tfrac{1}{3}P)Q_\perp \tag{23}$$

where P, the polarisation fraction, is defined experimentally as

$$P = \frac{I_\parallel - I_\perp}{I_\parallel + I_\perp}. \tag{24}$$

$I_\parallel$ and $I_\perp$ are the intensities of radiation observed with the electric vector parallel and perpendicular to the direction of the incident electron beam respectively. In the case of 2p excitation P may be defined theoretically in terms of the ratio of the cross section for excitation (both direct and cascade) to the magnetic $m_l = 0$ and $|m_l| = 1$ sublevels.

In our view the most thorough intermediate-energy measurements of the 1s-2s integrated cross section are those of Kauppila *et al* (1970). The actual experimentally observed parameter was not the flux of Lyman-α photons emitted from the quenching region but a ratio of this flux to the flux emitted from the collision region. Since the photon detectors were positioned at 90° to both the incident electron and hydrogen atom beams the measured ratio was

$$R_\perp = \frac{Q_\perp(2s)}{Q_\perp(2p)}. \tag{25}$$

In the following we describe how we determined this ratio using our theoretically evaluated 2s and 2p cross sections.

Considering initially the 1s-2s component it is clear from (23) that

$$Q_\perp(2s) = \frac{3}{3 - P} Q(2s) \tag{26}$$

where $Q(2s)$ is the cross section for the combination of both direct excitation *and* cascade into the 2s state. Denoting these by $Q(1s\text{-}2s)$ and $Q^{casc}(2s)$ respectively the above expression reduces to

$$Q_\perp(2s) = 0.903(Q(1s\text{-}2s) + Q^{casc}(2s)) \tag{27}$$

where we have used the theoretical value of $P = -0.323$ calculated by Casalese and Gerjuoy (1969) which is effectively in agreement with the experimentally determined value of -0.30 ± 0.02 (Ott *et al* 1970).

An expression similar to (26) exists for the $Q_\perp(2p)$ cross section. In this case P, which must theoretically take into account the m_l sublevel population of the 2p state by both direct and cascade excitation, has never been calculated. However Ott *et al* (1970) have measured P for 2p decay over the entire intermediate energy range. Substituting (27) into (25) and using the expression for $Q_\perp(2p)$ we obtain

$$R_\perp = \frac{0.903(Q(1s\text{-}2s) + Q^{casc}(2s))}{[3/(3 - P)](Q(1s\text{-}2p) + Q^{casc}(2p))} \tag{28}$$

where $Q(1s\text{-}2p)$ and $Q^{casc}(2p)$ refer to the integrated cross section for direct and cascade excitation to the 2p state respectively and P is the experimentally determined polarisation fraction. Of course both $Q(1s\text{-}2s)$ and $Q(1s\text{-}2p)$ are, along with $Q(1s\text{-}1s)$, the major results of this work. Note however that the calculation of $R_\perp$ also requires the cascade contributions which must be obtained by other means.

Using the transition probability data of Bethe and Salpeter (1957) it is found that the contributions to the 2s and 2p cascade cross sections are given by

$$Q^{casc}(2s) = 0.12Q(1s\text{-}3p) + 0.05Q(1s\text{-}4s) + 0.12Q(1s\text{-}4p) + 0.03Q(1s\text{-}4d) + 0.064Q(1s\text{-}5s) + 0.12Q(1s\text{-}5p) + 0.04Q(1s\text{-}5d) \quad (29)$$

$$Q^{casc}(2p) = Q(1s\text{-}3s) + Q(1s\text{-}3d) + 0.58Q(1s\text{-}4s) + 0.04Q(1s\text{-}4p) + 0.75Q(1s\text{-}4d) + 0.44Q(1s\text{-}5s) + 0.06Q(1s\text{-}5p) + 0.67Q(1s\text{-}5d) \quad (30)$$

where we assume that cascade contributions are only significant from states up to and including $n = 5$ and $l = 2$. The $Q(1s\text{-}nl)$ terms refer to cross sections for direct excitation to the nl level of the hydrogen atom.

Callaway *et al* (1987) have calculated the integrated cross sections for excitation to the $n = 3$ levels of hydrogen. Agreement of their results with the elastic and $n = 2$ cross sections of this work suggests that their $n = 3$ cross sections should also be reasonably accurate. Cross sections of similar accuracy are not available for excitation to the $n = 4$ and $n = 5$ levels. For these processes we shall use the results of Morrison and Rudge (1966). By interpolating the $n = 3$ cross sections of Callaway *et al* and the $n = 4$ and 5 cross sections of Morrison and Rudge to the energies at which our $n = 2$ cross sections were calculated, $R_\perp$ was evaluated. Figure 7 compares our theoretical results† with the experiments of Kauppila *et al* (1970). Agreement is good at the low- and high-energy limits but our results are high in the mid-range. Also included in this figure are theoretical values of $R_\perp$ which would be obtained if cascade effects were ignored. From this it is clear that cascade contributions have a small but significant

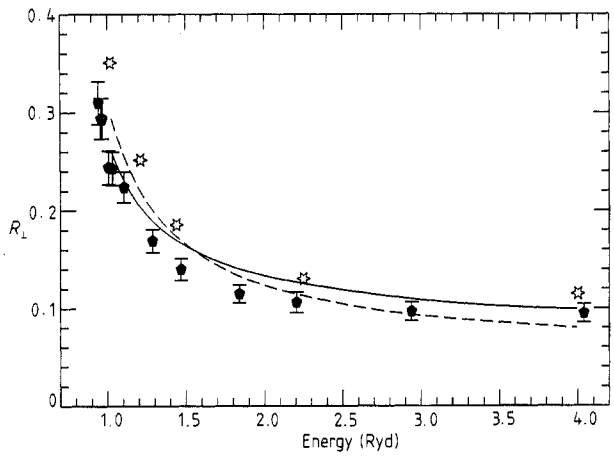

Figure 7. $R_\perp = Q_\perp(2s)/Q_\perp(2p)$. Full curve, this work; broken curve, this work ignoring cascade; six point stars, 1s-2s-2p close-coupling including cascade, Kingston *et al* (1976); full pentagons, Kauppila *et al* (1970). Error bars represent 2 standard deviations.

† Interpolated from calculations at the seven different energies defined in table 5.

effect. Cascade corrections are added to the 1s-2s-2p close-coupling results of Kingston *et al* (1976) and plotted for comparison. Given that this method takes no account of the infinite number of channels open at intermediate energies it is not surprising that agreement with experiment is poor. In figure 8 the experimental $Q(1s\text{-}2s)$ cross section derived from the $R_\perp$ results of Kauppila *et al* (1970) is presented. These experimental results are obtained by multiplying the $R_\perp$ by the experimental $Q_\perp(2p)$ measured by Long *et al* (1968) and then correcting for cascade and polarisation. Like most integrated cross section measurements the relative data obtained by Long *et al* required normalisation. Using the theoretical 1s-2p cross section of van Wyngaarden and Walters (1986b) along with the value of polarisation given experimentally by Ott *et al* (1970) and the interpolated cascade contribution of Morrison and Rudge (1966) the 2p expression equivalent to (26) was used to normalise the experimental value of $Q_\perp(2p)$ to 0.4615 πa_0^2 at 200 eV. This normalised cross section was then interpolated to the energies at which $R_\perp$ was measured in order to obtain the experimental 1s-2s cross section presented in figure 8. It is clear from this figure that our theoretical cross sections lie slightly above but within the 2 standard deviation error bars of the experimental measurements at most energies. The small discrepancy may arise from a slight error in the normalisation of the $Q_\perp(2p)$ results of Long *et al* or the inclusion of inaccurate cascade contributions. However, given these uncertainties overall agreement between experiment and theory is quite good.

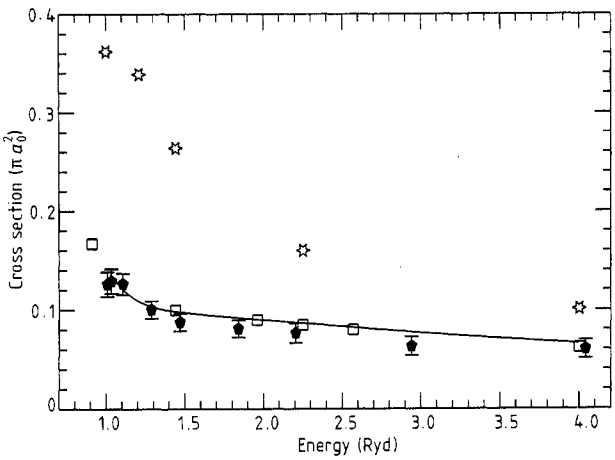

Figure 8. Integrated 1s-2s cross section. Full curve, this work (interpolated values); open squares, Callaway *et al* (1987); six point stars, 1s-2s-2p close-coupling, Kingston *et al* (1976); full pentagons, combination of Kauppila *et al* (1970) and Long *et al* (1968) with cascade removed (see text). Error bars represent 2 standard deviations.

The experimental 1s-2p cross section data of Long *et al* (1968) are presented in figure 9 along with three sets of theoretical results which were presented in figure 6. As already stated Long *et al* measured relative values of $Q_\perp(2p)$. The actual cross section is related to these measurements by

$$Q(1s\text{-}2p) = (1 - P/3)Q_\perp(2p) - Q^{casc}(2p) \tag{31}$$

where the normalisation of $Q_\perp(2p)$ is described in the previous paragraph. The polarisation fraction P has been measured by Ott *et al* (1970) and as in the case of 2s scattering the cascade contribution was evaluated using $n = 3$ cross sections from

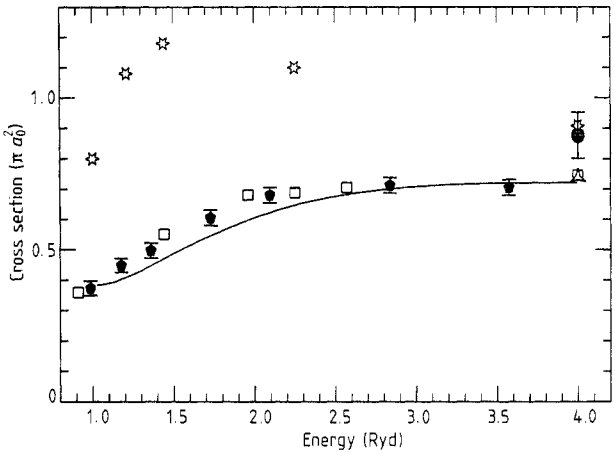

Figure 9. Integrated 1s–2p cross section. Symbols in common with figure 8 have the same meaning except the full pentagons which are Long *et al* (1968) normalised to theory at 200 eV and with cascade removed; full circle, Williams (1981). Error bars represent 2 standard deviations. Three point star at 4 Ryd, van Wyngaarden and Walters (1986b).

Callaway *et al* (1987) and $n=4$ and 5 excitation cross sections from Morrison and Rudge (1966). As with the $R_\perp$ parameter agreement of our results with experiment is good at the low- and high-energy limits but here we lie about 10% low in the mid-region. From (28) it is clear that this will cause $R_\perp$ to be high in the mid-region as we have already found. The mid-region discrepancy could be due to the inclusion of inaccurate cascade contributions or inaccurate experimental polarisation values in (31) but at present this cannot be verified. Also plotted in figure 9 is the absolute measurement of Williams (1981) at 4 Ryd. While this measurement agrees with the simple three-state 1s–2s–2p close-coupling approximation, it is very clearly in disagreement with the three more sophisticated calculations of van Wyngaarden and Walters (1986a, b), Callaway *et al* (1987) and the present work, which all support one another. There can be no doubt that these three calculations are superior to the 1s–2s–2p close-coupling results. We therefore concur with van Wyngaarden and Walters (1986a, b) that the absolute measurement is in significant disagreement with reliable theories, further experimental work is required to resolve this discrepancy.

In tables 4 and 5 we give our cross sections $Q(0\text{-}f)$ calculated from the amplitude (17)†. These are compared with cross sections $Q^*(0\text{-}f)$ evaluated without the second

Table 4. Integrated cross section for elastic scattering in πa_0^2. Q(1s–1s) is our final result. Q^*(1s–1s) refers to calculations which omit the corrections of § 2.3.2.

Energy (Ryd)	1.213	1.470	1.699	1.954	2.205	3.675
Energy (eV)	16.51	20.00	23.12	26.59	30.00	50.00
Q(1s–1s)	4.3587	3.4496	2.9245	2.4685	2.1295	1.1044
Q^*(1s–1s)	4.1942	3.3223	2.8093	2.3649	2.0357	1.0470

† The smooth curves shown in figures 7 to 9 come from smooth interpolation of these cross sections. This interpolation can be performed very accurately since, although our final cross sections are calculated only at six or seven discrete energies, we are able to evaluate the greater part of these cross sections, coming from uncorrected (see § 2.3.2) T-matrix elements in the range $0 \leq L \leq L_{max}$, on a very much finer grid.

Table 5. Integrated cross sections for excitation πa_0^2. Q(1s-2s) and Q(1s-2p) are our final results. Q^*(1s-2s) and Q^*(1s-2p) refer to calculations which omit the corrections of § 2.3.2. Call(1s-2s) and Call(1s-2p) are the work of Callaway *et al* (1987).

Energy (Ryd)	1.0200	1.2100	1.4400	2.2500	2.5725	2.9400	4.0000
Energy (eV)	13.877	16.463	19.592	30.612	35.000	40.000	54.421
Q(1s-2s)	0.1370	0.1087	0.0986	0.0867	0.0823	0.0775	0.0661
Q^*(1s-2s)	0.1400	0.1090	0.0954	0.0782	0.0736	0.0692	0.0599
Call(1s-2s)	—	—	0.100	0.085	0.080	—	0.062
Q(1s-2p)	0.3828	0.4092	0.4705	0.6466	0.6820	0.7054	0.7210
Q^*(1s-2p)	0.4080	0.4720	0.5550	0.7155	0.7392	0.7513	0.7441
Call(1s-2p)	—	—	0.551	0.688	0.705	—	0.746

Born corrections of § 2.3.2 for omitted states, i.e. from the amplitude (10), and with the results of Callaway *et al* (1987). Table 5 shows that the omitted state corrections of § 2.3.2 increase 1s-1s elastic cross section by 4-5%. From table 5 we see that the corrections increase the 1s-2s cross section by about 10% at higher energies but have much less effect close to the ionisation threshold. However, for 1s-2p scattering the corrections decrease the cross section by up to 15% just above the ionisation threshold. It is noteworthy that our uncorrected 1s-2p cross section, Q^*(1s-2p), is in better agreement with the results of Callaway *et al* than our corrected cross section Q(1s-2p). This is, perhaps, not surprising since Callaway *et al* made no attempt to correct for target states not included in their pseudostate set.

To conclude this section we consider the total cross section Q_T. This is obtained by applying the optical theorem to the imaginary part of the forward elastic amplitude. Our results are shown in figure 10 where they are compared with the values obtained by Callaway *et al* (1987). The agreement is very good.

Subtracting our elastic cross section Q(1s-1s) from Q_T we obtain the total inelastic cross section Q_T^{inel}. This is shown in figure 11 where it is compared with the total $n=2$ cross sections, i.e. Q(1s-2s)+Q(1s-2p). We see from the comparison that approximately half of all the inelastic flux is lost into channels other than 2s and 2p. This

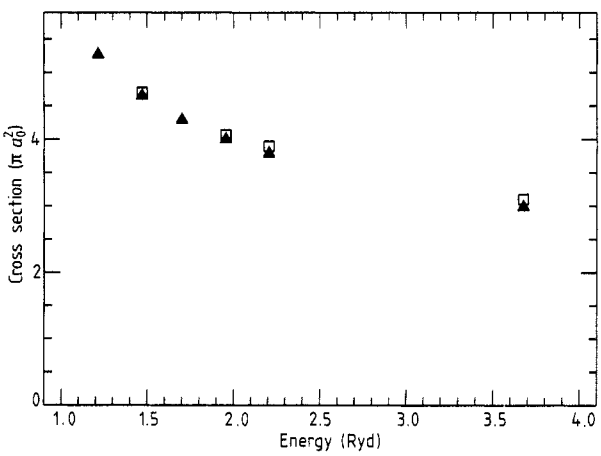

Figure 10. Total cross section Q_T. Full triangles, this work; open squares, Callaway *et al* (1987).

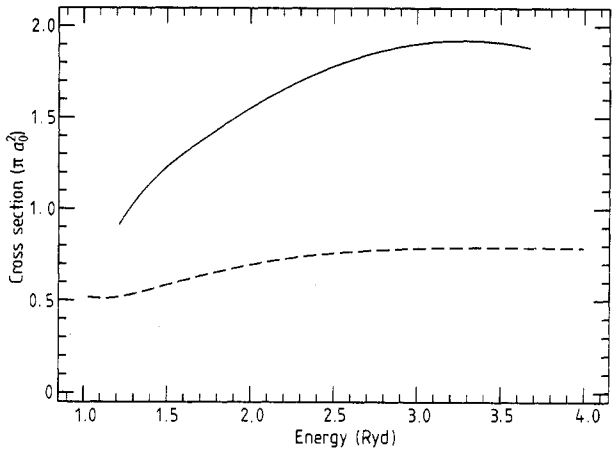

Figure 11. Comparison of the total inelastic cross section Q_T^{inel} (full curve) with the cross section for excitation to the $n = 2$ levels (broken curve). Both plots are interpolated values.

emphasises the point that these other channels must be properly taken into account in any theory which attempts to yield accurate results for intermediate-energy electron-hydrogen-atom scattering.

4. Conclusions

We have presented intermediate energy 1s, 2s and 2p electron-hydrogen-atom scattering calculations based upon the IERM theory of Burke *et al* (1987) which we believe to be the most extensive and accurate yet undertaken. We have obtained quite good agreement with the earlier theoretical work of Callaway *et al* (1987). This agreement is particularly good for the 1s-2s transition but is less satisfactory for 1s-2p where we attribute the differences to the neglect by Callaway *et al* of corrections for target states not included in their pseudostate set. Agreement with the normalised experimental data of Long *et al* (1968) and Kauppila *et al* (1970) is reasonably good for 1s-2s and 1s-2p scattering except that our 1s-2p results lie about 10% lower in the 1.2 to 2.5 Ryd region. We have confirmed the 1s-2p cross section calculated by van Wyngaarden and Walters (1986a) at 54.4 eV, thus casting further doubt upon the absolute measurement of Williams (1981). Clearly further absolute measurements of electron-hydrogen integrated cross sections are desirable, particularly because of the importance of these cross sections in many applications.

In following papers we shall report differential cross sections and electron-photon correlation parameters for 2p excitation. Rate coefficients derived from the cross sections of the present paper are to be published (Scholz *et al* 1989).

Acknowledgments

The majority of these calculations were carried out on the CRAY X-MP/48 at the Atlas Centre with the aid of a grant from SERC and analysed on our local Vax 11/750 also supported by SERC. We express gratitude to Dr D J Lennon and Dr K A

Berrington for their advice in using these facilities. One of us (TS) acknowledges with thanks the award of a Queen's University Postgraduate Scholarship.

References

Bethe H A and Salpeter E E 1957 *Quantum Mechanics of One and Two Electron Atoms* (Berlin: Springer)
Bransden B H, McCarthy I E, Mitroy J D and Stelbovic A T 1985 *Phys. Rev.* A **32** 166-75
Burke P G, Berrington K A and Sukumar C V 1981 *J. Phys. B: At. Mol. Phys.* **14** 289-305
Burke P G and Mitchell J F B 1973 *J. Phys. B: At. Mol. Phys.* **6** 207-303
Burke P G, Noble C J and Scott M P 1987 *Proc. R. Soc.* A **410** 289-310
Burke P G and Robb W D 1975 *Adv. At. Mol. Phys.* **11** 143-214
Burke P G, Schey H M and Smith K 1963 *Phys. Rev.* **129** 1258-1274
Buttle P J A 1967 *Phys. Rev.* **160** 719-29
Callaway J 1985 *Phys. Rev.* A **32** 775-83
Callaway J, Unnikrishnan K and Oza D H 1987 *Phys. Rev.* A **36** 2576-84
Casalese J and Gerjuoy E 1969 *Phys. Rev.* **180** 327-8
Fon W C, Berrington K A, Burke P G and Kingston A E 1981 *J. Phys. B: At. Mol. Phys.* **14** 1041-51
Kauppila W E, Ott W R and Fite W L 1970 *Phys. Rev.* A **1** 1099-108
Kingston A E, Fon W C and Burke P G 1976 *J. Phys. B: At. Mol. Phys.* **9** 605-18
Kingston A E and Walters H R J 1980 *J. Phys. B: At. Mol. Phys.* **13** 4633-62
Long R L Jr, Cox D M and Smith S J 1968 *J. Res. NB ST* A **72** 521-35
McDonald F A and Nuttall J 1969 *Phys. Rev. Lett.* **23** 361-3
Morrison D J T and Rudge M R H 1966 *Proc. Phys. Soc.* **89** 45-53
Noble C J and Nesbet R K 1984 *Comput. Phys. Commun.* **33** 399-411
Ott W R, Kauppila W E and Fite W L 1970 *Phys. Rev.* A **1** 1089-98
Reinhardt W P 1979 *Comput. Phys. Commun.* **17** 1-21
Schlessinger L and Schwartz C 1966 *Phys. Rev. Lett.* **16** 1173-4
Scholz T, Scott P and Burke P G 1988 *J. Phys. B: At. Mol. Opt. Phys.* **21** L139-45
Scholz T, Walters H R J, Burke P G and Scott M P 1989 *Mon. Not. R. Astron. Soc.* to be published
Slim H A and Stelbovics A T 1987 *J. Phys. B: At. Mol. Phys.* **20** L211-5
van Wyngaarden W L and Walters H R J 1986a *J. Phys. B: At. Mol. Phys.* **19** L53-8
—— 1986b *J. Phys. B: At. Mol. Phys.* **19** 929-68
—— 1986c *J. Phys. B: At. Mol. Phys.* **19** 1827-42
Walters H R J 1984 *Phys. Rep.* **116** 1-102
Williams J F 1981 *J. Phys. B: At. Mol. Phys.* **14** 1197-217